

Electric field intensity measurement by using doublet electromagnetically induced transparency of cold Rb Rydberg atoms

Ting Gong(宫廷), Shuai Shi(师帅), Zhonghua Ji(姬中华), Guqing Guo(郭古青), Xiaocong Sun(孙小聪),Yali Tian(田亚莉), Xuanbing Qiu(邱选兵), Chuanliang Li(李传亮), Yanting Zhao(赵延霆), and Suotang Jia(贾锁堂)
Citation: Chin. Phys. B, 2023, 32 (**10**): 103202. DOI: 10.1088/1674-1056/acf120
Journal homepage: http://cpb.iphy.ac.cn; http://iopscience.iop.org/cpb

What follows is a list of articles you may be interested in

Atom-based power-frequency electric field measurement using the radio-frequency-modulated Rydberg spectroscopy

Weixin Liu(刘伟新), Linjie Zhang(张临杰), and Tao Wang(汪涛)
Chin. Phys. B, 2023, 32 (**5**): 053203. DOI: 10.1088/1674-1056/aca6db

High-precision three-dimensional Rydberg atom localization in a four-level atomic system

Hengfei Zhang(张恒飞), Jinpeng Yuan(元晋鹏), Lirong Wang(汪丽蓉), Liantuan Xiao(肖连团), and Suo-tang Jia(贾锁堂)
Chin. Phys. B, 2021, 30 (**5**): 053202. DOI: 10.1088/1674-1056/abd46f

Dissipative preparation of multipartite Greenberger-Horne-Zeilinger states of Rydberg atoms

Chong Yang(杨崇), Dong-Xiao Li(李冬啸), and Xiao-Qiang Shao(邵晓强)
Chin. Phys. B, 2021, 30 (**2**): 023201. DOI: 10.1088/1674-1056/abd755

Precise measurement of a weak radio frequency electric field using a resonant atomic probe

Liping Hao(郝丽萍), Yongmei Xue(薛咏梅), Jiabei Fan(樊佳蓓), Jingxu Bai(白景旭), Yuechun Jiao(焦月春), Jianming Zhao(赵建明)
Chin. Phys. B, 2020, 29 (**3**): 033201. DOI: 10.1088/1674-1056/ab6c49

Tunable multistability and nonuniform phases in a dimerized two-dimensional Rydberg lattice

Han-Xiao Zhang(张焓笑), Chu-Hui Fan(范楚辉), Cui-Li Cui(崔淬砺), Jin-Hui Wu(吴金辉)
Chin. Phys. B, 2020, 29 (**1**): 013204. DOI: 10.1088/1674-1056/ab5d06

Electric field intensity measurement by using doublet electromagnetically induced transparency of cold Rb Rydberg atoms

Ting Gong(宫廷)[1,2,3], Shuai Shi(师帅)[1], Zhonghua Ji(姬中华)[2,3,†], Guqing Guo(郭古青)[1], Xiaocong Sun(孙小聪)[1], Yali Tian(田亚莉)[1], Xuanbing Qiu(邱选兵)[1], Chuanliang Li(李传亮)[1], Yanting Zhao(赵延霆)[2,3], and Suotang Jia(贾锁堂)[2,3]

[1] *Shanxi Engineering Research Center of Precision Measurement and Online Detection Equipment, School of Applied Science, Taiyuan University of Science and Technology, Taiyuan* 030024, *China*

[2] *State Key Laboratory of Quantum Optics and Quantum Optics Devices, Institute of Laser Spectroscopy, Shanxi University, Taiyuan* 030006, *China*

[3] *Collaborative Innovation Center of Extreme Optics, Shanxi University, Taiyuan* 030006, *China*

(Received 19 June 2023; revised manuscript received 5 August 2023; accepted manuscript online 17 August 2023)

We demonstrate a simple method to measure electric field intensity by using doublet electromagnetically induced transparency (EIT) spectra of cold Rb Rydberg atoms, where the frequency of the coupling laser does not need to be locked. Based on the Stark splitting of the Rb Rydberg state, $10D_{3/2}$, under electric fields and the corresponding calculated polarizabilities, the real electric field intensity is calculated using the difference in radio-frequency diffraction between two acousto-optic modulators, which acts as a frequency criterion that allows us to measure the electrical field without locking the coupling laser. The value measured by this simple method shows a good agreement with our previous work [*Opt. Express* **29** 1558 (2021)] where the frequency of the coupling laser needs to be locked with an additional EIT spectrum based on atom vapor and a proportional–integral–differential feedback circuit. Our presented method can also be extended to the measurement of electric field based on hot Rydberg atom vapor, which has application in industry.

Keywords: doublet electromagnetically induced transparency (EIT), Aulter–Townes (AT) splitting, Rydberg atom, electric field measurement

PACS: 32.60.+i, 32.10.Dk, 32.80.Ee, 42.50.Gy **DOI:** 10.1088/1674-1056/acf120

1. Introduction

Fast and intriguing developments in the behavior of cold atoms and molecules have been reviewed in numerous articles.[1,2] External electric field control of cold atoms and molecules is of special interest. In atomic configurations, it has been verified that one can obtain a small dipole moment under the action of an external electric field.[3] In molecular systems, a polar molecule possesses a permanent electric dipole moment along its interatomic axis. The dipole moment can be modified by an electric field, which can be used to measure the fundamental physical constants and pave the way for quantum computing and quantum simulation.[4–6] Thus, in order to control the interaction of atoms and molecules with electric fields and to address their characteristics precisely, it is necessary to know the actual electric field intensity that they really feel.

Atom-based field measurement has the potential to outperform traditional methods due to the stability, high sensitivity, self-calibration and intrinsic accuracy of atomic properties.[7–9] In particular, the Rydberg atom has been proven to be capable of measuring electric field and RF strength due to its large polarizabilities and microwave-transition dipole moments.[10–14] By sensing the electric field inside a vacuum chamber using cold Rydberg atoms, the stray electric field around a magneto-optical trap (MOT) can be shielded.[15] Then by measuring the Stark splitting of a cold Rydberg Rb atom, the electric field intensity can be calibrated, which is necessary for further calculating the permanent electric dipole moment of the cold ground-state polar molecule.[16]

An all-optical sensing method based on Rydberg electromagnetically induced transparency (EIT) is usually used to measure the electric field intensity because of the non-destructive detection mechanism. In general, the Rydberg EIT spectrum is observed by scanning the frequency of a probe (coupling) laser with an acousto-optic modulator (AOM), where the frequencies of both probe laser and coupling laser need to be locked by various techniques,[17,18] such as saturated absorption spectroscopy (SAS), EIT spectroscopy or Pound–Drever–Hall spectroscopy, etc. However, these frequency locking techniques need to be implemented in an elaborate experimental setup that may require expensive equipment and potentially timing sequence control. Thus developing a method without the requirement of frequency locking is meaningful for Rydberg atom-based field measurement.

In this paper, cold Rydberg Rb atoms are utilized to measure the electric field intensity in the region of an MOT by using doublet EIT spectroscopy. The AOM's ratio frequency diffraction is used as a frequency standard to enable measurement of the frequency shift of the Rydberg energy level under an external electric field. We calculate the polarizabilities of

†Corresponding author. E-mail: jzh@sxu.edu.cn

© 2023 Chinese Physical Society and IOP Publishing Ltd

sublevels of the Rydberg state and investigate the dependence of Stark splitting on the electric field. Finally, the electric field intensity is calibrated with a ratio of 0.79(3) relative to the set value, which shows good agreement with our previous work,[16] which needed additional equipment for the EIT spectrum setup and proportional–integral–differential (PID) components.

2. Experimental setup

The energy level and scheme of the experimental setup are displayed in Figs. 1(a) and 1(b), respectively. Our experiment is operated in an Rb MOT with a temperature of around 100 μK and a background pressure of 1×10^{-6} Pa. The magnetic gradient generated by a pair of anti-Helmholtz coils is about 15 G·cm^{-1}. The trapping and repumping laser are provided by two external-cavity diode lasers (Toptica DL100) and locked by SAS. The frequency of the trapping laser is red-detuned by 15 MHz by AOM1 from the transition of $5S_{1/2}$ $(F = 3) \rightarrow 5P_{3/2}$ $(F' = 4)$; the repumping laser is resonant with $5S_{1/2}$ $(F = 2) \rightarrow 5P_{3/2}$ $(F' = 3)$. The probe laser is generated from the trapping laser and tuned to the $5S_{1/2}$ $(F = 3) \rightarrow 5P_{3/2}$ $(F' = 4)$ transition by AOM2. The coupling laser is a home-made diode laser with a scanning frequency that drives the transition $5P_{3/2}$ $(F = 4) \rightarrow 10D_{3/2}$ with the central frequency of 515.1718 nm. The probe laser and coupling laser are coupled into two optical fibers, overlapped, counter-propagated and focused onto cold Rb atoms with a radius of 40 μm for both. The powers of the probe laser and coupling laser are 0.6 μW and 1 mW, respectively. Wavelength monitoring by a wavemeter helps to tune the frequency of the coupling laser to the transition between the excited state, $|e\rangle$, and the desired Rydberg state, $|r\rangle$. Two electrode meshes with a size of 2 cm × 4 cm are placed inside the vacuum chamber and 4.8 cm apart. The diameter of the central trapped cold atoms is around 100 μm. The relative sizes of electrode meshes and atoms mean that the two electrode meshes can be regarded as parallel-plate electrodes. In a DC electric field, the $10D_{3/2}$ Rydberg state will split into two sublevels: $10D_{3/2,1/2}$ and $10D_{3/2,3/2}$.

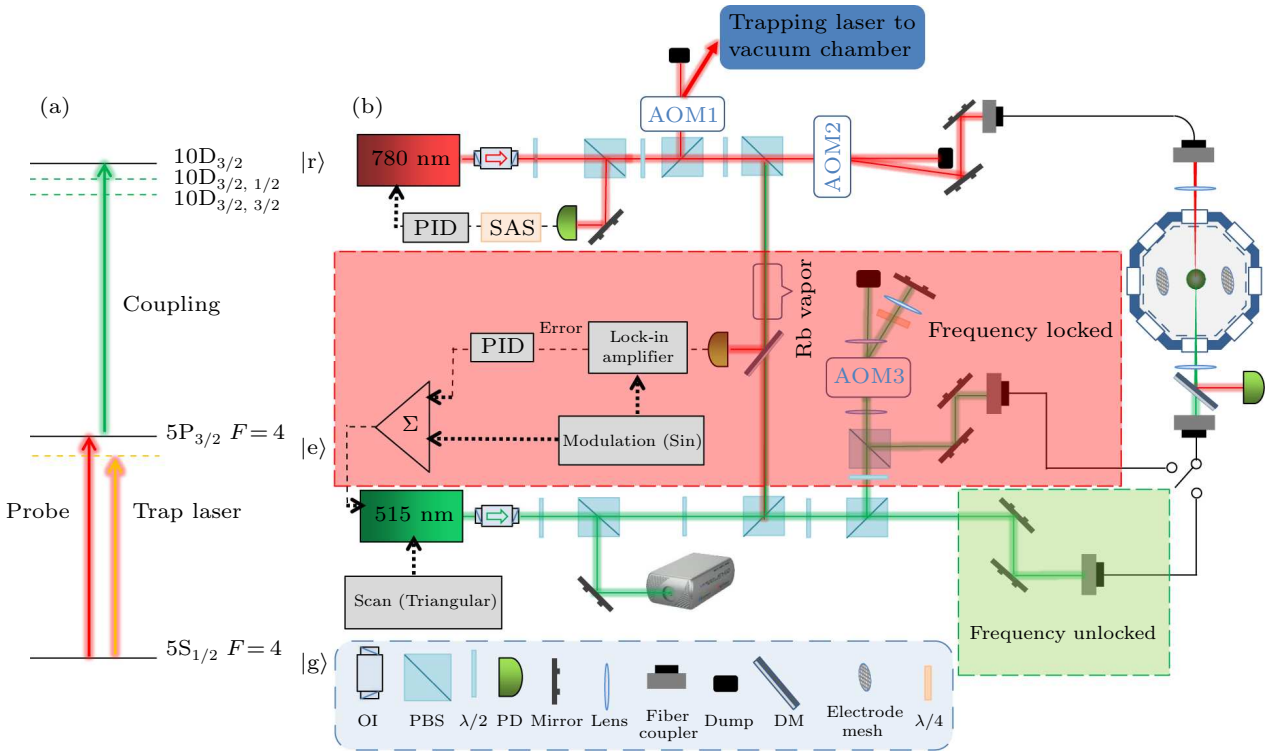


Fig. 1. Energy level diagram of the Rb ladder system (a) and scheme of the experimental setup (b). The probe laser is generated from the Rb trapping laser by AOM2, which is tuned to the $5S_{1/2}$ $(F = 3) \rightarrow 5P_{3/2}$ $(F' = 4)$ transition; the trapping laser is red-detuned by 15 MHz from this transition by AOM1. The coupling laser is scanned through $5P_{3/2}$ $(F' = 4)$ to the $10D_{3/2}$ state by applying a triangular-wave voltage to the piezoelectric transducer (PZT) of the laser. The frequency-locked probe laser and frequency-scanning coupling laser are counter-propagated and focused onto cold Rb atoms with a radius of 40 μm. The EIT spectrum is obtained by detecting the transmission of the probe laser using a photodiode (PD). Two electrode meshes, 4.8 cm apart, are placed in vacuum chamber to make the Rydberg state $10D_{3/2}$ split into the two sublevels $10D_{3/2,1/2}$ and $10D_{3/2,3/2}$ in an electric field.

When the frequency of the probe laser is resonant with the lower transition ($|g\rangle \rightarrow |e\rangle$), the absorption of the probe laser will be suppressed in the presence of a near-resonance coupling laser. By scanning the frequency of the coupling laser, the EIT spectrum can be obtained by measuring the transmission of the probe laser with a photodiode (PD) after a dichroic mirror (DM). To scan the frequency of the coupling laser, a complex setup shown in the red shaded area in Fig. 1(b) was

needed in our previous work,[16] while in this work we only need to use the simple setup shown in the green shaded area. In the scheme of red shaded area, the frequency of the coupling laser is locked by the Rydberg EIT spectrum in a vapor cell with a PID feedback and scanned by a double-passed AOM. To improve the diffraction efficiency of the AOM, a pair of lenses can also be added. In the scheme of the green shaded area, the frequency scanning of the coupling laser is realized by applying an internal voltage to the PZT using a triangular wave. The scanning rate of the PZT is fixed during the whole experimental process. Unlike the scheme of the red shaded area, there is no need for a complex frequency locking mechanism for the pumping laser in the scheme of the green shaded area, and there is also no complex timing sequence control, which is needed in Ref. [16].

3. Results and discussion

By scanning the frequency of the coupling laser, we obtain the spectrum shown in Fig. 2(a), called the doublet EIT spectrum. It is different from the traditional EIT spectrum, which only has one resonance peak. The two peaks observed here are caused by the high Rabi frequency of the trapping laser. The existence of a trapping laser leads to the Aulter–Townes (AT) splitting of the $|g\rangle$ state and $|e\rangle$ state, which leads to two EIT resonance peaks when scanning the frequency of the coupling laser. It is observed that the amplitudes of the two peaks of the doublet EIT spectrum are asymmetric, which is because the probe laser is not resonant with the transition $|g\rangle \rightarrow |e\rangle$ with the effect of AT splitting.[19] We fit the experimental data by using a bimodal Lorentz function, shown by the red curve in Fig. 2(a). By changing the power of the trapping laser, we find that the interval between the two peaks increases with increasing laser power, as shown in Fig. 2(b).

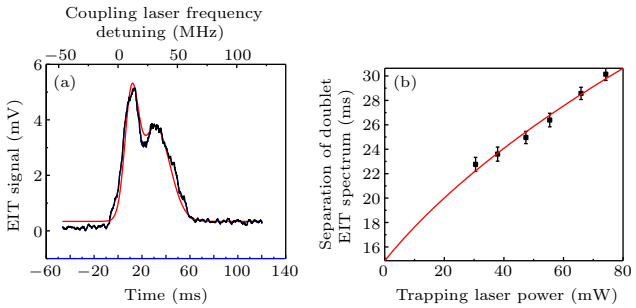


Fig. 2. (a) Doublet EIT spectrum as a function of the coupling laser detuning. (b) The relationship between trapping laser power and the separation of the doublet EIT spectrum.

The frequency of the coupling laser is proportional to the voltage on the PZT, and it is scanned by applying a triangular-wave voltage as a function of time, $V(t)$; thus the spectrum obtained in Fig. 2(a) is in fact directly related to time, shown as the bottom horizontal coordinate. The corresponding frequency interval of the scanning range, which is proportional to corresponding time interval, is derived as follows. In Fig. 2(a) the interval of two peaks in units of time represents the AT splitting and depends on the power of the trapping laser with the relationship $\Delta_t = k_1\sqrt{k_2 P_{trap} + \delta_t^2}$,[16] where k_1 is the ratio of Δ_t to the corresponding frequency interval Δ_f, k_2 is a fitting coefficient, P_{trap} is the trapping laser power and δ_t is the detuning of the trapping laser relative to $5S_{1/2}$ $(F = 3) \rightarrow 5P_{3/2}$ $(F' = 4)$ with the known value of 15 MHz (determined by the frequency difference of AOM1 and AOM2). Using this equation to fit the measured data in Fig. 2(b), shown by the red curve, we obtain that $k_1 = 9.9(7) \times 10^{-4}$ s·MHz^{-1} and $k_2 = 9(2)$ MHz$^2 \cdot$ mW^{-1}. Through the ratio value, k_1, we can easily transform the data of the bottom horizontal coordinate in units of time in Fig. 2(a) to the corresponding frequency value, shown as the top horizontal coordinate in Fig. 2(a). Here, the frequency interval of doublet EIT spectra under a certain trapping laser power can be regarded as a frequency reference standard.

As mentioned before, by applying a DC electric field, the energy level of the $10D_{3/2}$ Rydberg state will split into two sublevels: $10D_{3/2,1/2}$ and $10D_{3/2,3/2}$. Here the DC electric field intensity is selected between 458 V·cm^{-1} from consideration of the spectral resolution to 625 V·cm^{-1} with the limitation of the maximum voltage of the power supply (3 kV). Figure 3 displays the DC Stark splitting of doublet EIT spectra in various electric fields. It contains four peaks: peak 1 (3) and peak 2 (4) are components of the $|m_J| = 3/2$ (1/2) sublevel, where $|m_J|$ is the absolute value of the projection quantum number along the electric field vector. Each component of the sublevels contains two resonance EIT spectra as we mentioned above. We can see that the intensity of the transmission resonant peaks of $|m_J| = 3/2$ is larger than that of $|m_J| = 1/2$ due to the larger transition electric dipole moment from $5P_{3/2}$ to $10D_{3/2,3/2}$. Here, the separation between peak 1 (3) and peak 2 (4) is called as the doublet EIT, and the separation between peak 1 (2) and peak 3 (4) is called the DC Stark splitting. By fitting the experimental data using a multipeak Lorenz function, we can obtain the resonance central frequencies. The central frequency difference between peak 1 and peak 3, f_{13}, is expected to be the same as the frequency difference between peak 2 and peak 4, f_{24}, which represents the separation of $10D_{3/2,3/2}$ and $10D_{3/2,1/2}$. After fitting the central frequencies of these four peaks, we derive f_{13} and f_{24} and take their average. Figure 4 shows the relationship between the DC electric field and the separation of $10D_{3/2,3/2}$ and $10D_{3/2,1/2}$. We can see that the separation increases with increasing electric field intensity.

The Stark shift of Rydberg atoms can be expressed as[20]

$$\Delta W = -\frac{1}{2}\alpha(bE)^2$$

$$= -\frac{1}{2}\left(\alpha_0 + \alpha_2 \frac{3m_J{}^2 - J(J+1)}{J(2J-1)}\right)(bE)^2, \qquad (1)$$

where J is the angular quantum number, α is the polarizability, α_0 is the scalar polarizability, which describes the average energy shift, and α_2 is the tensor polarizability, which stands for Stark level splitting. E is the set electric field intensity, which is the quotient of the set voltage and the distance between the electrode meshes. As the intensity of an actual DC electric field is not equal to the applied DC electric field, a parameter b is introduced here as the ratio between the real electric field intensity felt by atoms and the electric field intensity we applied to the electrode meshes. Once the parameter b is obtained, the real electric field intensity felt by atoms can be derived from bE.

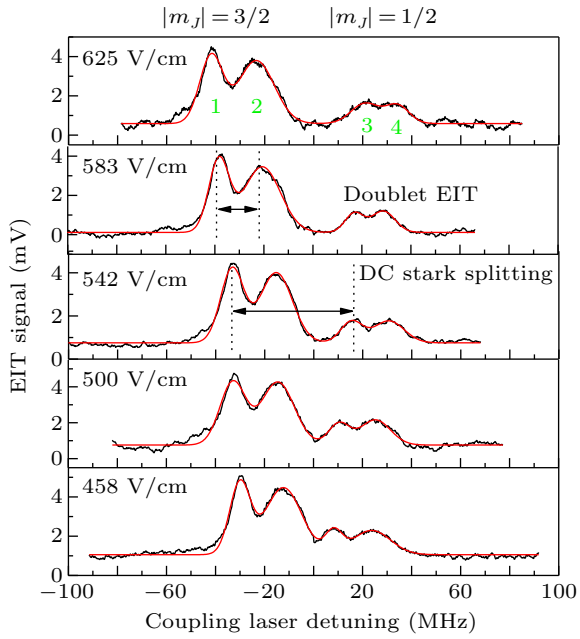


Fig. 3. DC Stark splitting of the doublet EIT spectra in different electric fields. By applying an external electric field, the Rydberg state $10D_{3/2}$ will split into $10D_{3/2,3/2}$ and $10D_{3/2,1/2}$. The red curve is the result of multipeak Lorenz fitting. Two doublet EIT spectra are generated from these two sublevels $|m_J| = 3/2$ and $|m_J| = 1/2$.

To estimate the electric field intensity felt by Rb Rydberg atoms, it is essential to calculate the scalar polarizability and tensor polarizability accurately. As noted in Ref. [21], α_0 and α_2 can be written as

$$\alpha_0 = \frac{2}{3}\sum_{n',l',J'} \frac{|\langle n',s',l',J'||\mu||n,s,l,J\rangle|^2}{(2J+1)[E(n',l',J') - E(n,l,J)]}, \qquad (2)$$

$$\alpha_2 = 2\left(\frac{10J(2J-1)}{3(2J+3)(J+1)(2J+1)}\right)^{1/2} \times \sum_{n',l',J'} \frac{|\langle n',s',l',J'||\mu||n,s,l,J\rangle|^2}{E(n',s',l',J') - E(n,s,l,J)} \times (-1)^{J+J'+1}\begin{Bmatrix} J & J' & 1 \\ 1 & 2 & J \end{Bmatrix}, \qquad (3)$$

where $\langle n',s',l',J'||\mu||n,s,l,J\rangle$ is the electric dipole matrix element. The transition should be allowed by the selection rules. $E(n,s,l,J)$ and $E(n',s',l',J')$ are the energies in the absence of the electric field. Because the polarizability is an overall effect with the consideration of the neighboring states, here we calculate it by setting n with a range of ± 5 and l up to 10. Finally, the polarizability is obtained with the value of 942.6 Hz·cm^2·V^{-2} for $|m_J| = 1/2$ and 1469.9 Hz·cm^2·V^{-2} for $|m_J| = 3/2$, which is consistent with the fitting results from the Atom calculator[22] (942.97 Hz·cm^2·V^{-2} for $|m_J| = 1/2$ and 1470.20 Hz·cm^2·V^{-2} for $|m_J| = 3/2$). We can see that the polarizability of $|m_J| = 3/2$ is larger than that of $|m_J| = 1/2$. This will give rise to a larger Stark shift, which makes the level $5P_{3/2}$ closer to $10D_{3/2,3/2}$ than to $10D_{3/2,1/2}$.

After acquiring the polarizability of sublevels, we can deduce their DC Stark splitting by using the relationship shown by Eq. (1). Using the difference in the frequency shifts of two substates is more accurate than estimating the frequency shift of each sublevel when the frequency of the coupling laser is scanning. Thus, we subtract the polarizability of $|m_J| = 3/2$ and $|m_J| = 1/2$ and fit the experimental data by using Eq. (1), as shown in Fig. 4 by the red solid curve. Here, b is set as a variable with a fitted value of 0.79(3). This means that the electric field intensity felt by the atom is 0.79(3) times that actually applied to the electrode meshes. This value is in accordance with our previous measurement,[16] where the frequency of the coupling laser needs to be locked by Rb Rydberg EIT in vapor[23] and scanned by a double-passed AOM. In contrast, the methods presented in this paper can not only obtain the same accuracy, but also make the experiment faster and easier to operate. Moreover, the method we propose has no system restriction and can be used in an atom vapor system. In an atom vapor system, an additional laser should be introduced in place of the trapping laser. This laser is divided into two beams by a polarizing beam splitter; one beam passes through an AOM and the other does not. The fixed frequency difference between these two beams can be treated as a frequency standard, which is realized by setting the radio frequency of the AOM. Since the intensity of the laser used here is much less than that of the trapping laser, there is no need to consider the AT splitting of the ground state and excited state.

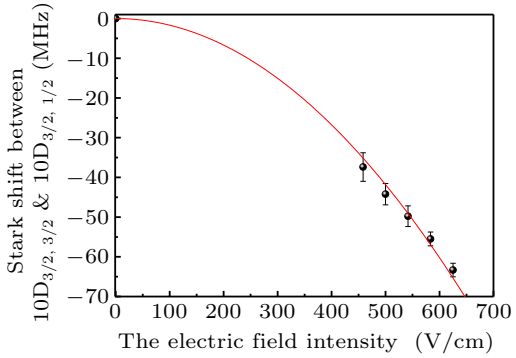


Fig. 4. Stark splitting between $10D_{3/2,3/2}$ and $10D_{3/2,1/2}$ sublevels versus electric field.

4. Conclusion

In this paper, we calibrate the DC electric field intensity by using Rydberg doublet EIT spectra, without a complex frequency locking scheme and timing sequence control. We treat the difference in two peaks in the doublet EIT spectrum as the frequency reference. By applying an electric field, the DC Stark effect is observed. The Stark splitting between sublevels of $10D_{3/2}$ is measured by scanning the frequency of the coupling laser. The polarizability of the $10D_{3/2}$ state is calculated, and is in good agreement with the theoretical results of other groups. Based on the calculated polarizability, we calibrate the electric field intensity applied to the meshes in the vacuum chamber. The calibration result is consistent with our previous measurement, where the laser is frequency-locked by additional EIT spectrum and scanned by a double-passed AOM and timing control is needed. Our proposed simple method can be used to calibrate the electric field intensity with a similar system and can be extended to an atom vapor system.

Acknowledgments

Project supported by the National Natural Science Foundation of China (Grant Nos. 12034012, 12074231, 12274272, and 61827824), Science and technology innovation plan of colleges and universities in Shanxi Province (Grant No. 2021L313), Science and Technology Project of State Grid (Grant No. 5700-202127198A-0-0-00), Fundamental Research Program of Shanxi Province (Grant No. 202203021222204), and Taiyuan University of Science and Technology Scientific Research Initial Funding (Grant Nos. 20222008 and 20222132).

References

[1] Julienne P S 2003 *Nature* **424** 24
[2] Ketterle W 2002 *Rev. Mod. Phys.* **74** 1131
[3] Lepers M, Li H, Wyart J F, Quéméner G and Dulieu O 2018 *Phys. Rev. Lett.* **121** 063201
[4] DeMille D 2002 *Phys. Rev. Lett.* **88** 067901
[5] Matsuda K, De Marco L, Li J R, Tobias W G, Valtolina G, Quéméner G and Ye J 2020 *Science* **370** 1324
[6] DeMille D, Doyle J M and Sushkov A O 2017 *Science* **357** 990
[7] Cronin A D, Schmiedmayer J and Pritchard D E 2009 *Rev. Mod. Phys.* **81** 1051
[8] Savukov I M, Seltzer S J, Romalis M V and Sauer K L 2005 *Phys. Rev. Lett.* **95** 063004
[9] Acosta V M, Jensen K, Santori C, Budker D and Beausoleil R G 2013 *Phys. Rev. Lett.* **110** 213605
[10] Frey M T, Ling X, Lindsay B G, Smith K A and Dunning F B 1993 *Rev. Sci. Instrum.* **64** 3649
[11] Osterwalder A and Merkt F 1999 *Phys. Rev. Lett.* **82** 1831
[12] Thiele T, Deiglmayr J, Stammeier M, Agner J A, Schmutz H, Merkt F and Wallraff A 2015 *Phys. Rev. A* **92** 063425
[13] Barredo D, Kübler H, Daschner R, Löw R and Pfau T 2013 *Phys. Rev. Lett.* **110** 123002
[14] Sedlacek J A, Schwettmann A, Kübler H, Löw R, Pfau T and Shaffer J P 2012 *Nat. Phys.* **8** 819
[15] Grabowski A, Heidemann R, Löw R, Stuhler J and Pfau T 2006 *Fortschr. Phys.* **54** 765
[16] Gong T, Ji Z H, Du J Q, Zhao Y T, Xiao L T and Jia S T 2021 *Opt. Express* **29** 1558
[17] Qin X T, Jiang Y, Ma W X, Ji Z H, Peng W X and Zhao Y T 2022 *Chin. Phys. B* **31** 064216
[18] Xu Z S, Wang H M, Cai M H, You S H and Liu H P 2022 *Chin. Phys. B* **31** 123201
[19] Zhang H, Wang L M, Chen J, Bao S X, Zhang L J, Zhao J M and Jia S T 2013 *Phys. Rev. A* **87** 033835
[20] Zimmerman M L, Littman M G, Kash M M and Kleppner D 1979 *Phys. Rev. A* **20** 2251
[21] Angel J R P and Sandars P G H 1968 *Proc. R. Soc. A.* **305** 125
[22] ibalić N, Pritchard J, Adams C and Weatherill K 2017 *Comput. Phys. Commun.* **220** 319
[23] Jiao Y C, Li J KK, Wang L M, Zhang H, Zhang L J, Zhao J M and Jia S T 2016 *Chin. Phys. B* **25** 053201